










ARTICLE

Emerging Technologies

Geographic distribution of feather $\delta^{34}\text{S}$ in Europe

Vojtěch Brlík^{1,2}  | Petr Procházka²  | Luana Bontempo³  |
 Federica Camin^{3,4,5}  | Frédéric Jiguet⁶  | Gergely Osváth^{7,8}  |
 Craig A. Stricker⁹  | Michael B. Wunder¹⁰  | Rebecca L. Powell¹¹ 

¹Department of Ecology, Charles University, Prague, Czech Republic

²Czech Academy of Sciences, Institute of Vertebrate Biology, Brno, Czech Republic

³Traceability Unit, Research and Innovation Centre, Fondazione Edmund Mach, Trento, Italy

⁴Center Agriculture Food Environment (C3A), University of Trento, San Michele all'Adige, Trentino, Italy

⁵International Atomic Energy Agency, Vienna International Centre, Vienna, Austria

⁶Museum National d'Histoire Naturelle, Sorbonne Université, CNRS, UMR7204 CESCO, Paris, France

⁷Museum of Zoology, Academic Cultural Heritage Department, Babeş-Bolyai University, Cluj-Napoca, Romania

⁸Evolutionary Ecology Group, Hungarian Department of Biology and Ecology, Babeş-Bolyai University, Cluj-Napoca, Romania

⁹U.S. Geological Survey, Fort Collins Science Center, Denver, Colorado, USA

¹⁰Department of Integrative Biology, University of Colorado Denver, Denver, Colorado, USA

¹¹Department of Geography and the Environment, University of Denver, Denver, Colorado, USA

Correspondence

Vojtěch Brlík

Email: vojtech.brlik@gmail.com

Funding information

Czech Science Foundation, Grant/Award Number: 20-00648S; Grant Agency of Charles University, Grant/Award Number: 254119; National Science Foundation, Grant/Award Number: DBI-1565128; Charles University, Grant/Award Number: UNCE 204069

Handling Editor: Julia A. Jones

Abstract

Geographic distribution models of environmentally stable isotopes (the so-called “isoscares”) are widely employed in animal ecology, and wildlife forensics and conservation. However, the application of isoscares is limited to elements and regions for which the spatial patterns have been estimated. Here, we focused on the ubiquitous yet less commonly used stable sulfur isotopes ($\delta^{34}\text{S}$). To predict the European $\delta^{34}\text{S}$ isoscare, we used 242 feather samples from Eurasian Reed Warbler (*Acrocephalus scirpaceus*) formed at 69 European wetland sites. We quantified the relationships between sample $\delta^{34}\text{S}$ and environmental covariates using a random forest regression model and applied the model to predict the geographic distribution of $\delta^{34}\text{S}$. We also quantified within-site variation in $\delta^{34}\text{S}$ and complementarity with other isotopes on both individual and isoscare levels. The predicted feather $\delta^{34}\text{S}$ isoscare shows only slight differences between the central and southern parts of Europe while the coastal regions were most enriched in ^{34}S . The most important covariates of $\delta^{34}\text{S}$ were distance to coastline, surface elevation, and atmospheric concentrations of SO_2 gases. The absence of a systematic spatial pattern impedes the application of the $\delta^{34}\text{S}$ isoscare, but high complementarity

Michael B. Wunder and Rebecca L. Powell contributed equally to this study.

This is an open access article under the terms of the [Creative Commons Attribution](https://creativecommons.org/licenses/by/4.0/) License, which permits use, distribution and reproduction in any medium, provided the original work is properly cited.

© 2023 The Authors. *Ecosphere* published by Wiley Periodicals LLC on behalf of The Ecological Society of America.

with other isoscapes advocates the combination of multiple isoscapes to increase the precision of animal tracing. Feather $\delta^{34}\text{S}$ compositions showed considerable within-site variation with highest values in inland parts of Europe, likely attributed to wetland anaerobic conditions and redox sensitivity of sulfur. The complex European geography and topography as well as using $\delta^{34}\text{S}$ samples from wetlands may contribute to the absence of a systematic spatial gradient of $\delta^{34}\text{S}$ values in Europe. We thus encourage future studies to focus on the geographic distribution of $\delta^{34}\text{S}$ using tissues from diverse taxa collected in various habitats over large land masses in the world (i.e., Africa, South America, or East Asia).

KEYWORDS

feather, isoscape, sulfur, wetland

INTRODUCTION

The stable isotopic compositions of ecosystem components vary spatially due to a wide variety of biogeochemical processes (West et al., 2010). These geographic distributions of isotopes (i.e., “isoscapes”) can be used to infer spatial origin and have manifold applications, especially in animal ecology, and wildlife forensics and conservation (Hobson & Wassenaar, 2018). Isoscapes are used to infer geographic space use and thus applied to study altitudinal migration (Villegas et al., 2016), to quantify the strength of migratory connectivity (Norris et al., 2006), or to trace the natal origins of animals (Brlík, Procházka, Hansson, et al., 2022; Procházka et al., 2013). The use of geographic space can affect animal fitness, and stable isotopes thus may indirectly inform demographic models to understand population changes and target conservation efforts (Jiguet et al., 2019). Continental-scale isoscapes essential for tracing origins are currently available for $\delta^2\text{H}$, $\delta^{13}\text{C}$, $\delta^{15}\text{N}$, $\delta^{18}\text{O}$, and $^{87}\text{Sr}/^{86}\text{Sr}$ but are mostly applied in regions with steep isotopic gradients or isotopically distinct regions (Amundson et al., 2003; Bataille et al., 2020; West et al., 2010).

Some isoscapes feature systematic spatial patterns on continental scales (e.g., $\delta^2\text{H}$ and $\delta^{18}\text{O}$ in North America and East Asia; Bowen & Revenaugh, 2003), while others show weaker spatial structure (e.g., $\delta^{13}\text{C}$ and $\delta^{15}\text{N}$ in Africa and South America; Amundson et al., 2003; Powell & Still, 2010) limiting their application. The weak spatial structure of isoscapes can be overcome by the combination of spatial predictions using multiple isoscapes or by optimization of sampling to increase the precision of tracing (e.g., Contina et al., 2022; Popa-Lisseanu et al., 2012; Veen et al., 2014). Either way, developing isotopic maps is essential for broadening the potential of isotopes in animal ecology and wildlife forensics.

Geographic distributions of stable sulfur isotopes ($\delta^{34}\text{S}$) in contemporary organic tissues have already been modeled for Great Britain, Tanzania, sub-Saharan Africa, and the conterminous United States (Brlík, Procházka, Hansson, et al., 2022; Kabalika et al., 2020; Newton, 2021; Valenzuela et al., 2011). Additionally, a recent study used archeological remains to predict the geographic distribution of $\delta^{34}\text{S}$ in Europe (Bataille et al., 2021). Moreover, deposition of marine-derived sulfates from coastal toward inland areas has been identified as the most important driver of $\delta^{34}\text{S}$ geographic distribution (Lott et al., 2003; Zazzo et al., 2011). Gradients formed by the deposition of marine sulfates have been detected on both regional (Wadleigh & Blake, 1999; Zazzo et al., 2011) and continental scales (Bataille et al., 2021; Brlík, Procházka, Hansson, et al., 2022; Valenzuela et al., 2011). In addition, spatial variation in atmospheric concentrations of combustion gases, as well as bedrock geochemistry, has also been found to affect the spatial patterns of $\delta^{34}\text{S}$ values (Case & Krouse, 1980; Thode, 1991). Indeed, detailed knowledge of these relationships could be used to predict $\delta^{34}\text{S}$ geographic distributions on continental scales. The isotopic offset between environment and organic tissues is generally low for $\delta^{34}\text{S}$ (Felicetti et al., 2003; Florin et al., 2011; McCutchan et al., 2003; Tcherkez & Tea, 2013), providing an opportunity to apply a single $\delta^{34}\text{S}$ isoscape to a range of taxa. Despite these benefits, continental $\delta^{34}\text{S}$ isoscapes of organic tissues are currently available only for part of North America and for human archeological remains in Europe (Bataille et al., 2021; Valenzuela et al., 2011).

In this study, we (1) develop a European $\delta^{34}\text{S}$ isoscape using feather keratin samples, (2) quantify within-site variation in $\delta^{34}\text{S}$, and (3) quantify the complementarity of $\delta^{34}\text{S}$ with other feather isotopes (individual level) and other isoscapes (geographic level).

METHODS

Sample collection

We used 242 feathers from Eurasian Reed Warbler (*Acrocephalus scirpaceus*) with known geographic origin at 69 European wetland sites previously used in Procházka et al. (2013; 94 individuals from 25 sites) and newly collected in 2019 (148 individuals from 44 sites; Figure 1). At these sites, we collected the innermost primary feathers from one to four juvenile Eurasian Reed Warblers (one sample = 8 sites; two = 2; three = 6; and four = 53) during the fledgling period (from early June to early August; Figure 1). Juveniles of the Eurasian Reed Warbler are mostly stationary during this period before post-fledging dispersal (Grinkevich et al., 2009; Mukhin, 2004), and we consider the sampling locations their natal origins and thus known geographic origins of these samples.

Isotopic analysis

We cleaned the feather samples in a 2:1 chloroform:methanol mixture to remove surface lipids and other contaminants, and air-dried the samples.

Feather vane material of about 300 µg encapsulated in tin capsules was then combusted using a Vario Isotope Cube Elemental Analyzer (Elementar, Germany). The resulting SO₂, CO₂, and N₂ gases were transferred to the isotope ratio mass spectrometer (visION, Elementar, Germany) via a continuous flow inlet system. Sample ³⁴S/³²S, ¹³C/¹²C, and ¹⁵N/¹⁴N ratios are expressed in delta notation (δ³⁴S, δ¹³C, and δ¹⁵N) in parts per mil (‰) relative to Vienna-Pee Dee Belemnite (V-PDB) for δ¹³C, Air for δ¹⁵N, and Vienna-Canyon Diablo Troilite (V-CDT) for δ³⁴S according to the following equation:

$$\delta^i E = \frac{R_{\text{sample}} - R_{\text{standard}}}{R_{\text{standard}}},$$

where the superscript *i* indicates the mass number of the heavier isotope of element *E* (e.g., ³⁴S) and *R* the isotope ratio of *E* (e.g., ³⁴S/³²S) in the sample and in the internationally recognized standard.

The values of δ³⁴S, δ¹³C, and δ¹⁵N were calculated against in-house standards that were calibrated against international reference materials using multipoint normalization: fuel oil NBS-22 (International Atomic Energy Agency [IAEA], Vienna, Austria; −30.03‰) and sugar IAEA-CH-6 (−10.45‰) for δ¹³C, L-glutamic acid

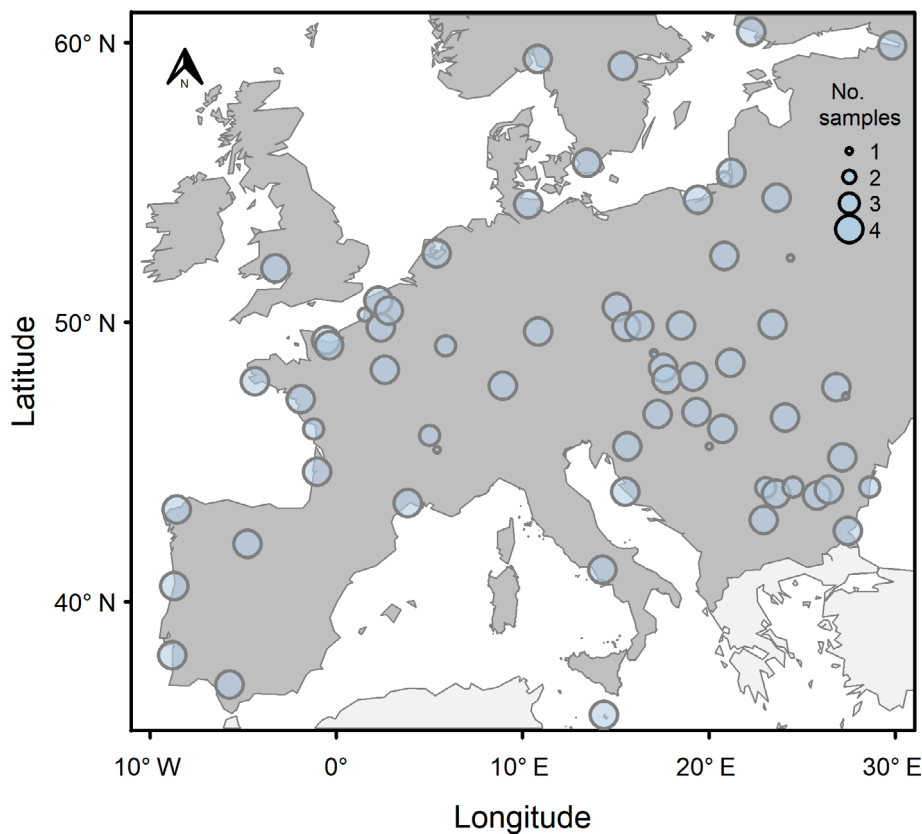


FIGURE 1 Locations of European sampling sites ($n = 69$) coinciding with the geographic origins of feather samples collected from juvenile Eurasian Reed Warblers (*Acrocephalus scirpaceus*; $n = 242$). Dark gray region depicts the extent of prediction.

USGS 40 (-26.39‰ and -4.5‰ for $\delta^{13}\text{C}$ and $\delta^{15}\text{N}$), hair USGS 42 ($\delta^{15}\text{N} = +8.05\text{‰}$, $\delta^{13}\text{C} = -21.09\text{‰}$, and $\delta^{34}\text{S} = +7.84 \pm 0.25\text{‰}$), and USGS 43 ($\delta^{15}\text{N} = +8.44\text{‰}$, $\delta^{13}\text{C} = -21.28\text{‰}$, and $\delta^{34}\text{S} = +10.46 \pm 0.22\text{‰}$) for $^{13}\text{C}/^{12}\text{C}$, $^{15}\text{N}/^{14}\text{N}$, and $^{34}\text{S}/^{32}\text{S}$, respectively, and barium sulfates IAEA-SO-5 and NBS 127 (IAEA) for $^{34}\text{S}/^{32}\text{S}$. Each sample was analyzed three times and we present its isotopic composition as an average value. Measurement error, calculated as one SD of internal laboratory standard measured 10 times, was $\pm 0.4\text{‰}$ for $\delta^{34}\text{S}$, $\pm 0.1\text{‰}$ for $\delta^{13}\text{C}$, and $\pm 0.2\text{‰}$ for $\delta^{15}\text{N}$. Stable isotope analyses were conducted in the Traceability Unit at the Research and Innovation Centre, Fondazione Edmund Mach, Italy.

Covariates of $\delta^{34}\text{S}$

We gathered geographic distributions of potential atmospheric, anthropogenic, geographical, and geological covariates of $\delta^{34}\text{S}$ values, including SO_2 atmospheric concentrations (Case & Krouse, 1980; Ohizumi & Fukuzaki, 1997), distance to coastline (Valenzuela et al., 2011; Zazzo et al., 2011), and bedrock age and type (Case & Krouse, 1980; Thode et al., 1953). Moreover, we extracted the geographic distribution of NO_2 atmospheric concentrations—tracing the intensity of various source combustion—and log human population density, which affects the intensity of fossil fuel combustion (Garg et al., 2001; Martin et al., 2003). We also included surface elevation as a covariate, as we expected depletion in ^{34}S with increasing elevation (atmospheric deposition), similar to the patterns observed in water isotopes (Dansgaard, 1954, 1964). The original spatial resolution and sources of covariate distribution layers are detailed in Table 1. Geographic distribution layers were assembled using Google Earth Engine, a cloud-based geospatial analysis platform (Gorelick et al., 2017).

Geostatistical analysis

We resampled the spatial resolution of all covariate layers to 2 km to match the scale of potential within-natal site movements of juvenile Eurasian Reed Warblers and extracted the covariate values for each sample at each sampling location. We calculated the average $\delta^{34}\text{S}$ values at sampling sites for further analysis ($n = 69$). To identify and quantify the relationships between covariates and average feather $\delta^{34}\text{S}$ at the sites, we employed a random forest regression model using the R package *caret* (Kuhn, 2008). Random forest models are based on a large number of regression trees grown using a randomly sampled subset of the training dataset (Belgiu & Dragut, 2016; Breiman, 2001). Random forest models can accommodate different data types including categorical covariates. This enabled us to predict abrupt changes in the spatial surfaces by avoiding smoothing over the regions (Bataille et al., 2018, 2021). We built the random forest model with 500 regression trees, randomly selecting two covariates at each node, and estimating model accuracy using leave-one-out cross-validation. In this process, each observation was withheld for subsequent validation of an entire random forest model, and this process was repeated for each observation (Vapnik, 1998). We derived the relative importance of individual covariates (index of node purity) and visualized the partial dependencies (relationships) of these covariates on $\delta^{34}\text{S}$. We then applied the final random forest regression model to covariate values per grid cell and predicted the geographic distribution of feather $\delta^{34}\text{S}$ values within the extent of prediction. Spatial autocorrelation of the residuals was assessed using Moran I statistics at distance classes ranging from 0 to 700 km. We present the predicted $\delta^{34}\text{S}$ isoscape for Europe $>31^\circ \text{N}$, $<61^\circ \text{N}$ excluding Greece and Turkey, and for elevations up to 750 m above sea level. These restrictions reflect the

TABLE 1 Covariates used for modeling the geographic distribution of feather $\delta^{34}\text{S}$ values from Eurasian Reed Warblers across Europe.

Covariate	Units	Year	Original resolution	Source
SO_2 atmospheric concentration	mol m^{-2}	2018	1 km	Copernicus Sentinel (2015a)
NO_2 atmospheric concentration	mol m^{-2}	2018	1 km	Copernicus Sentinel (2015b)
Human density	$\log(\text{persons km}^{-2})$	2010	0.8 km	CIESIN (2018)
Distance to coastline	km	—	1 km	NASA Ocean Biology Processing Group (2012)
Surface elevation	m above sea level	—	0.8 km	Danielson and Gesch (2011)
Bedrock type ^a	nominal (class)	—	Discrete	Pawlewicz et al. (2003)
Bedrock age ^a	nominal (years)	—	Discrete	Pawlewicz et al. (2003)

^aLayers were derived from vector layers with a scale of 1:5,000,000.

geographic range of sampling sites and their upper range of elevations (Figure 1).

Similarly, we quantified the relationships between the within-site SD of $\delta^{34}\text{S}$ values and the covariates. We calculated within-site SD for each sampling site with at least three $\delta^{34}\text{S}$ values (total of 230 samples from 59 sites) and employed the random forest regression model as detailed above. Finally, we quantified the relationship between average within-site $\delta^{34}\text{S}$ values and within-site SDs of $\delta^{34}\text{S}$ values using Pearson's correlation coefficients.

Complementarity of $\delta^{34}\text{S}$ with other isotopes

We assessed the complementarity of $\delta^{34}\text{S}$ on individual and isoscape levels. On the individual level, we quantified Pearson's correlations between feather $\delta^{34}\text{S}$ values, and the feather $\delta^{13}\text{C}$ and $\delta^{15}\text{N}$ values measured in Eurasian Reed Warblers ($n = 242$). Similarly, we assessed isoscape-level complementarity to identify similarities among spatial patterns of isoscapes. We compared spatial patterns using per-grid-cell Pearson's correlation coefficients between the predicted $\delta^{34}\text{S}$ isoscape and the previously known feather-based $\delta^2\text{H}$ and $\delta^{13}\text{C}$ isoscapes. At both individual and isoscape levels, low correlations indicate high level of complementarity.

For assessing the complementarity on the isoscape level, we prepared the European feather $\delta^2\text{H}$ isoscape. We extracted $\delta^2\text{H}$ in precipitation from Global Network of Isotopes in Precipitation and applied a geospatial model to predict the $\delta^2\text{H}$ isoscape using precipitation, average temperature, surface elevation, and absolute latitude as independent explanatory variables via a web-based computing platform IsoMAP (Bowen et al., 2014; Brlík, Procházka, Bontempo, et al., 2022). We calibrated the resulting isoscape of $\delta^2\text{H}$ in precipitation using the equation $\delta^2\text{H}_{\text{feather}} = 1.28 \times \delta^2\text{H}_{\text{precipitation}} - 10.29$ to account for discrimination between precipitation and feather $\delta^2\text{H}$ in the Eurasian Reed Warbler derived by Procházka et al. (2013), and resampled to the spatial resolution of the predicted feather $\delta^{34}\text{S}$ isoscape.

Similarly, we prepared the European plant $\delta^{13}\text{C}$ isoscape by combining climatic (Abatzoglou et al., 2018), land cover (Buchhorn et al., 2020), and crop production layers (Yu et al., 2020). We adapted the process described in Powell et al. (2012, 2019) using Google Earth Engine. We accounted for an assumed plant–feather discrimination by adding +2‰ to the plant $\delta^{13}\text{C}$ isoscape (Hobson et al., 2012) and resampled to the spatial resolution of the predicted feather $\delta^{34}\text{S}$ isoscape. Analyses were conducted in R 4.1.2 (R Core Team, 2021).

RESULTS

Geographic distribution of $\delta^{34}\text{S}$ and main covariates

The predicted feather $\delta^{34}\text{S}$ isoscape features a region depleted in ^{34}S over eastern Great Britain, Benelux, Germany, Poland, and northern Ukraine. In contrast, northern Europe (i.e., Norway, Denmark, Sweden, Finland, and the Baltic states) and western to southern Europe (i.e., the Iberian Peninsula, France, Italy, the Balkans, Romania, and Bulgaria), together with the European coastline, were more enriched in ^{34}S (Figure 2).

The most important covariates of $\delta^{34}\text{S}$ values were distance to coastline, surface elevation, and atmospheric concentrations of SO_2 (Figure 3). The relationships between the covariates and the $\delta^{34}\text{S}$ values were (1) negative (depletion in ^{34}S) for distance to coastline, surface elevation, and human density; (2) positive (enrichment in ^{34}S) for bedrock age; and (3) more complex for atmospheric concentrations of SO_2 and NO_2 (Figures 3 and 4).

Overall, the cross-validation of the random forest regression model explained 15% of variance (slope = 0.8, SE = 0.3, $p = 0.01$, intercept = 0.4, SE = 1.0, $p = 0.67$) and root mean square error of the final model was 6.1‰, representing 14% of the range of the $\delta^{34}\text{S}$ in the training dataset (Appendix S1). We did not find spatial autocorrelation in residuals of the random forest regression model (Moran I test p values >0.05 for all distance classes).

Within-site variation in $\delta^{34}\text{S}$

The average within-site variation (SD) in feather $\delta^{34}\text{S}$ was 2.1‰ (median = 1.3, min = 0.1, first quartile = 0.7, third quartile = 2.5, max = 9.1). Overall, the highest within-site variation was detected in some inland parts of Europe (i.e., France, Germany, Hungary, southern Poland), while the lowest values appeared in coastal regions (Figure 5). The correlation between the within-site averages and within-site SDs was -0.2 (Pearson's correlation), but statistically not different from zero (95% CI = -0.44 , 0.06; $p = 0.13$), and sites close to the coastline tended to show low within-site variability ($\rho = 0.27$; 95% CI = 0.02, 0.51; $p = 0.03$). Based on leave-one-out cross-validation, the random forest regression model of within-site variability explained only 1% of variation (slope = 0.3, SE = 0.4, $p = 0.45$, intercept = 1.4, SE = 0.9, $p = 0.20$; Appendix S2). Root mean square error of the model was 1.6‰, representing 18% of the range of the values in the training dataset. Due to the low performance of the model, we did not predict the geographic

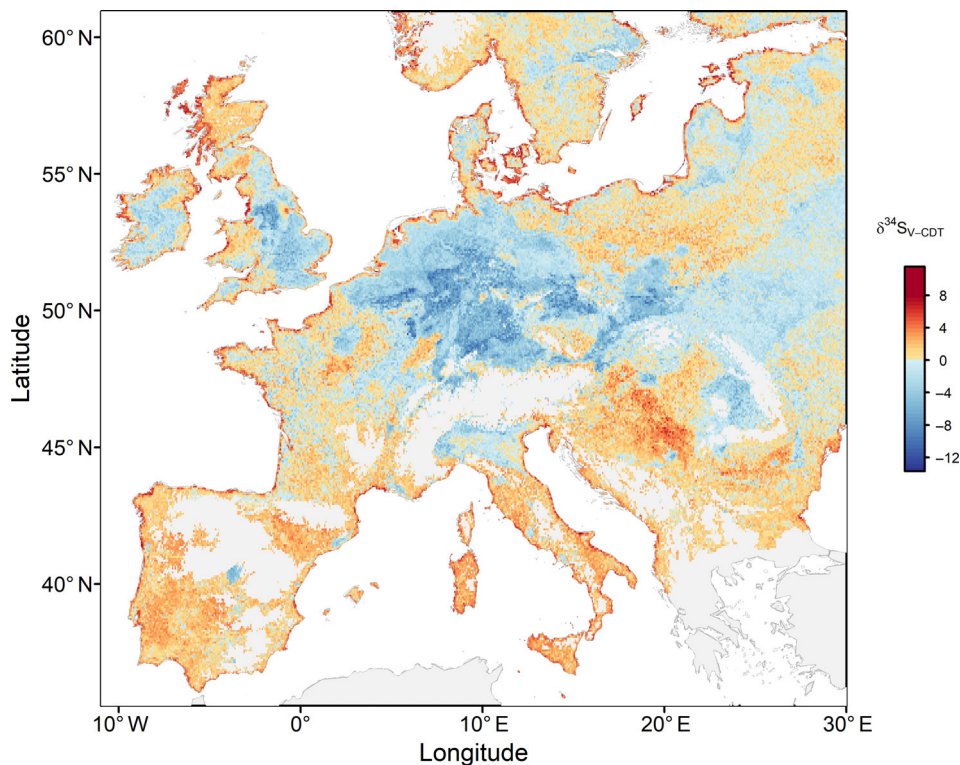


FIGURE 2 The predicted geographic distribution of $\delta^{34}\text{S}$ values in Europe derived using Eurasian Reed Warbler feather samples of known spatial origin; gray color represents regions outside prediction range.

distribution of within-site variability across Europe and only present raw values (Figure 5).

Complementarity of $\delta^{34}\text{S}$ with other isotopes

The feather $\delta^{34}\text{S}$ values ranged between -27.6‰ and 20.4‰ (mean = 1.0, SD = 8.5, $n = 242$), $\delta^{13}\text{C}$ values ranged between -28.9‰ and -11.5‰ (mean = -23.9 , SD = 2.1, $n = 242$) and $\delta^{15}\text{N}$ values ranged between 6.5‰ and 25.6‰ (mean = 12.6, SD = 2.7, $n = 242$). The feather $\delta^{34}\text{S}$ values were weakly related to both $\delta^{13}\text{C}$ ($\rho = 0.29$; 95% CI = 0.17, 0.40) and $\delta^{15}\text{N}$ ($\rho = -0.19$; 95% CI = -0.30 , -0.06 ; Figure 6). We also identified only weak relationships of the predicted feather European $\delta^{34}\text{S}$ isoscape with the feather $\delta^2\text{H}$ ($\rho = 0.19$) or feather $\delta^{13}\text{C}$ isoscapes ($\rho = 0.01$; Figure 7).

DISCUSSION

We predicted the geographic distribution of $\delta^{34}\text{S}$ values in Europe using feather samples of known geographical origin. The $\delta^{34}\text{S}$ isoscape shows high $\delta^{34}\text{S}$ values along the European coast and only slight differences in

$\delta^{34}\text{S}$ values between the central and southern parts of Europe. The $\delta^{34}\text{S}$ values also varied highly within sites, especially in inland parts of Europe. In the absence of a systematic spatial pattern, the $\delta^{34}\text{S}$ isoscape, derived from feathers grown in wetlands, appears to be of limited use alone. However, its high level of complementarity with other isoscapes or an optimization of sampling (Contina et al., 2022) could increase animal tracing precision using this tool.

Geographic distribution and main covariates of $\delta^{34}\text{S}$

Given the coastal regions are the most enriched in ^{34}S , our prediction that the distance to coastline is a key covariate of the geographic distribution of $\delta^{34}\text{S}$ is in line with previous studies (Amrani et al., 2013; Fry, 2006; Zazzo et al., 2011). The inland parts of Europe showed only slight differences in $\delta^{34}\text{S}$ values between the interior regions that have been predicted or shown in previous studies using various techniques and predictors to model isoscapes (Bataille et al., 2021; Brlík, Procházka, Hansson, et al., 2022; Newton, 2021; Valenzuela et al., 2011; Wadleigh & Blake, 1999). Among the explanations for the absence of a systematic spatial pattern across Europe could

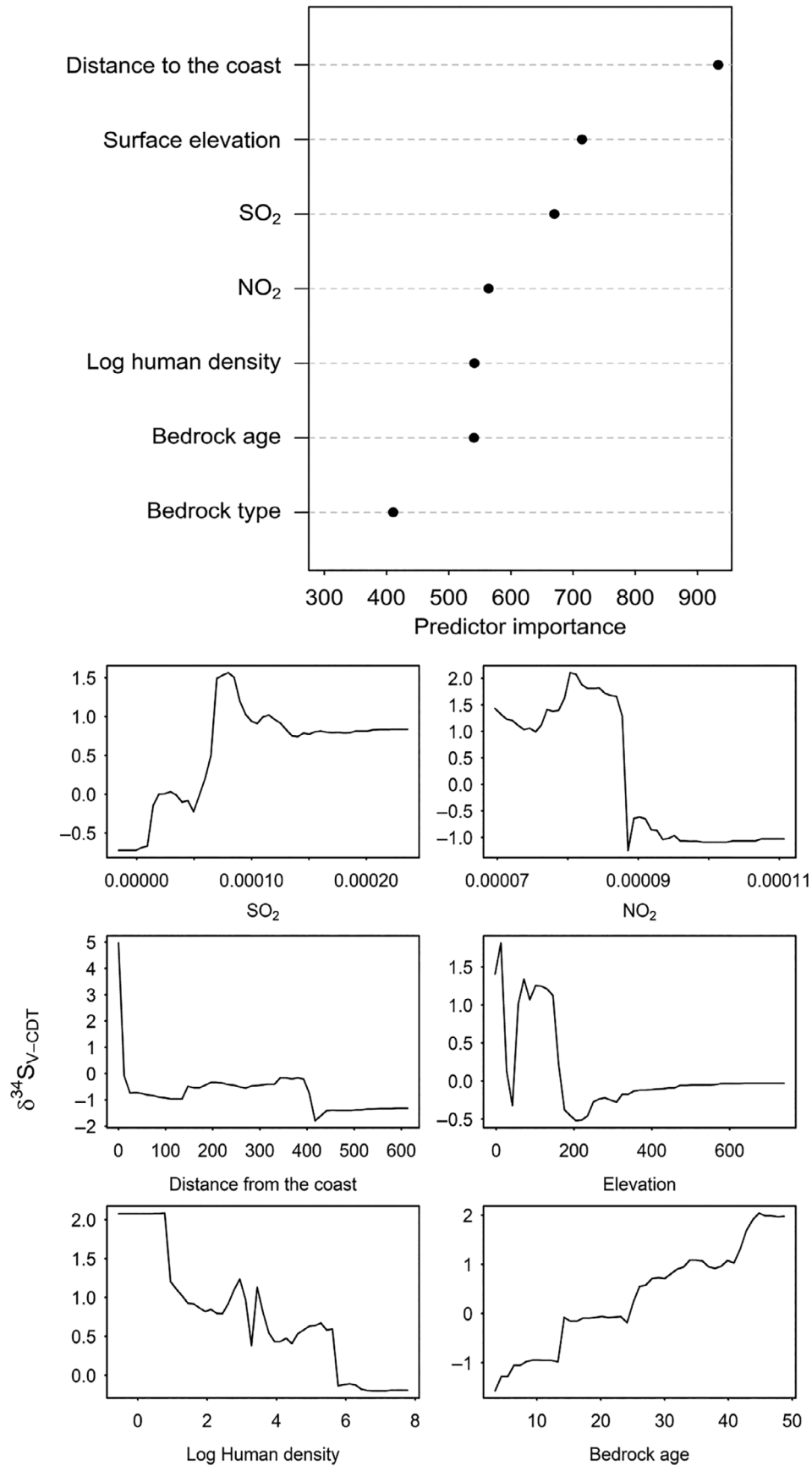


FIGURE 3 Relative importance of covariates (top) and partial dependencies of $\delta^{34}\text{S}$ on covariates (bottom) based on the Eurasian Reed Warbler feather samples of known spatial origin in Europe.

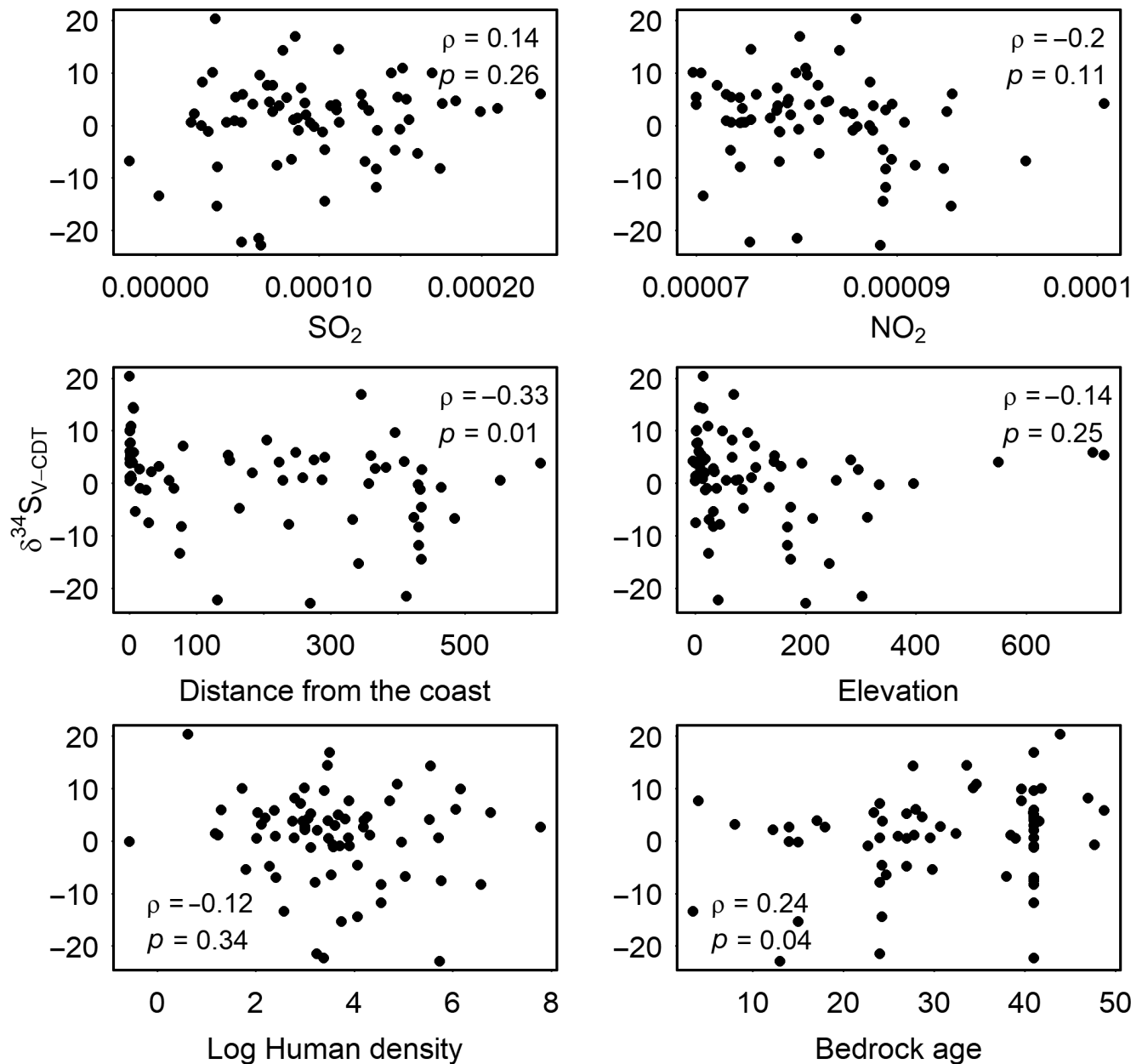


FIGURE 4 Relationships between $\delta^{34}\text{S}$ values and predictors ($n = 69$) based on the Eurasian Reed Warbler feather samples of known spatial origin in Europe.

be: (1) the complex geography of the European continent, (2) the spatial clustering of human population and related spatial distribution of fossil fuel combustion intensity, and (3) the effect of variability in redox state of wetland soils that influences tissue $\delta^{34}\text{S}$ isotopic compositions.

The transportation of marine sulfate aerosols creates the coast–inland gradient of $\delta^{34}\text{S}$ values on regional and continental scales (Valenzuela et al., 2011; Zazzo et al., 2011). However, the European continent has complex coastal geography, intersected by mountain ranges, and contains regions with distinct climates (Beck et al., 2018) and

variable patterns (Troen & Petersen, 1989). Complex geography and wind systems could thus disrupt inland transportation of marine sulfates, partly explaining the patchiness of the predicted $\delta^{34}\text{S}$ isoscape. This explanation would be indirectly supported by the presence of a $\delta^{34}\text{S}$ gradient over homogeneous land masses in North America (Valenzuela et al., 2011) or sub-Saharan Africa (Brlík, Procházka, Hansson, et al., 2022; Procházka et al., 2018). However, our explanation lacks direct support and even contradicts the recent European $\delta^{34}\text{S}$ isoscape that shows a continent-wide coast–inland gradient of $\delta^{34}\text{S}$ values within Europe. We note, however, that the previous study

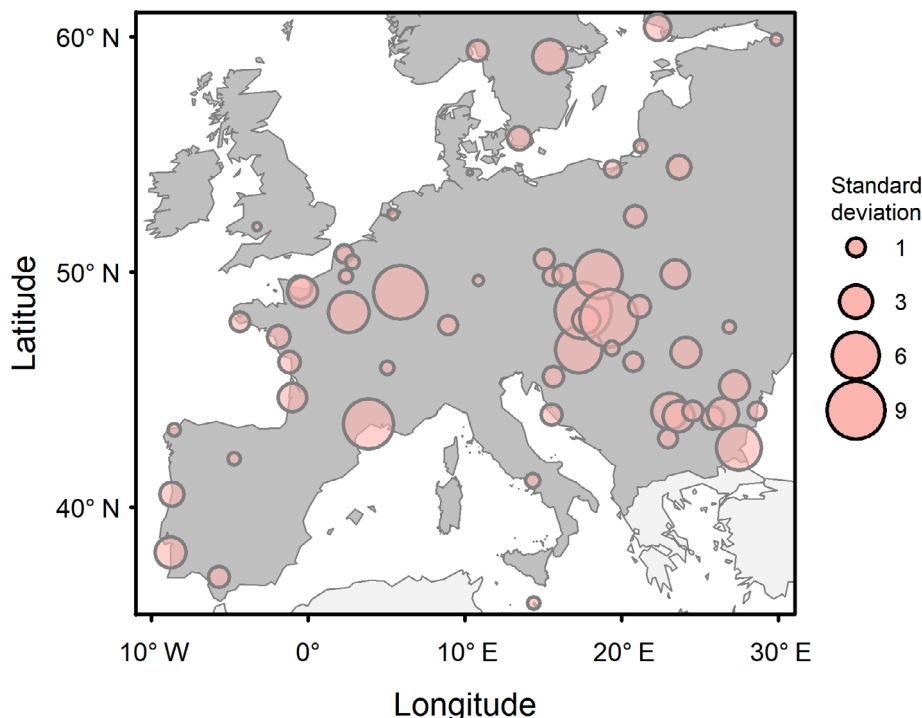


FIGURE 5 Within-site variability presented as SDs of Eurasian Reed Warbler feather $\delta^{34}\text{S}$ values at sites with at least three samples collected (59 sites).

used a different combination of predictor variables, mostly based on archeological and historical collagen samples (Bataille et al., 2021).

Human populations have boomed in the past century, along with the intensity of anthropogenic activities, which have influenced atmospheric concentrations of combustion gases (i.e., SO_2 and NO_2) that we identified as important covariates of $\delta^{34}\text{S}$ values. Human population and related anthropogenic sources of these gases are, however, spatially clustered with numerous local peaks (e.g., in urban agglomerations and around factories) and highest densities in the central and western parts of Europe. The clustered geographic distribution of these covariates could further disrupt the coast–inland gradient of $\delta^{34}\text{S}$ values caused by marine-derived sulfate aerosols (Rees et al., 1978; Zazzo et al., 2011) and result in patchiness of the predicted feather $\delta^{34}\text{S}$ isoscape.

Another factor related to the overall patchiness of the predicted feather $\delta^{34}\text{S}$ isoscape could be the biological conditions in wetlands—the breeding habitat of the Eurasian Reed Warbler and the only habitat we sampled. Wetlands store water and accumulate organic material and nutrients from surrounding areas. Consequently, geochemical conditions in a wetland may be affected by the catchment capacity of water reservoirs, which collect waters leaching various bedrocks in the surrounding region. Moreover, high availability of nutrients and low oxygen levels support development

of anaerobic conditions (Cherry, 2011) and associated bacterial communities. These bacteria affect $\delta^{34}\text{S}$ composition through fractionation against ^{34}S , resulting in substantial depletion in ^{34}S in solid-phase sulfur-bearing minerals such as pyrite (Chambers & Trudinger, 1979; Thode, 1991). Unfortunately, the anaerobic conditions in wetlands cannot be predicted from remote sensing imagery and are thus difficult to quantify on continental scales. Finally, the predicted feather $\delta^{34}\text{S}$ isoscape considers the relationships identified within wetland sampling sites but applies these relationships to predict $\delta^{34}\text{S}$ values over Europe, potentially leading to bias (e.g., due to the absence of low redox conditions in terrestrial habitats).

Within-site variation in $\delta^{34}\text{S}$

We found large differences in within-site $\delta^{34}\text{S}$ variation, with the highest values detected at some inland sites in Europe. In contrast, coastal sites showed mostly low variation, which could be explained by the prevailing effect of marine-derived sulfates with uniform $\delta^{34}\text{S}$ values (Rees et al., 1978). Within-site variation in $\delta^{34}\text{S}$ also tended to increase with increasing distance to coastline, likely due to reduced transport of marine sulfates and an increasing impact of low redox conditions in wetland environments (Chambers & Trudinger, 1979; Thode, 1991), which could vary locally, both between

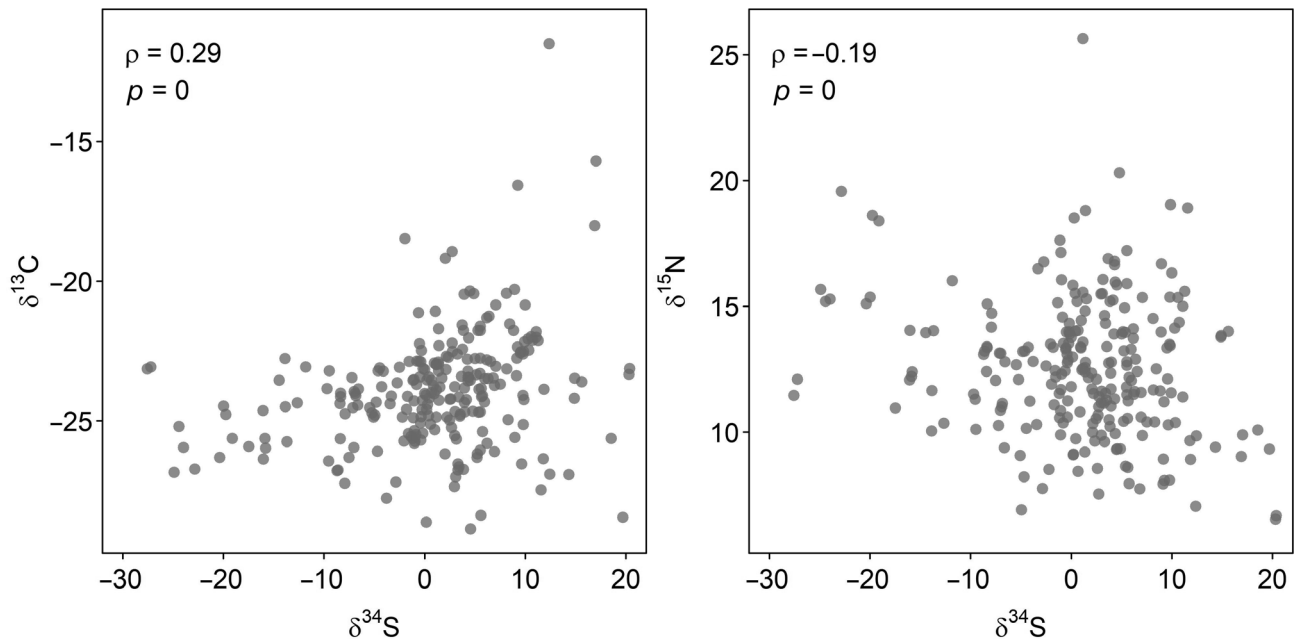


FIGURE 6 Relationship between Eurasian Reed Warbler feather $\delta^{34}\text{S}$ and $\delta^{13}\text{C}$ (left) and $\delta^{34}\text{S}$ and $\delta^{15}\text{N}$ (right) measurements ($n = 242$) including Pearson's correlation coefficients.

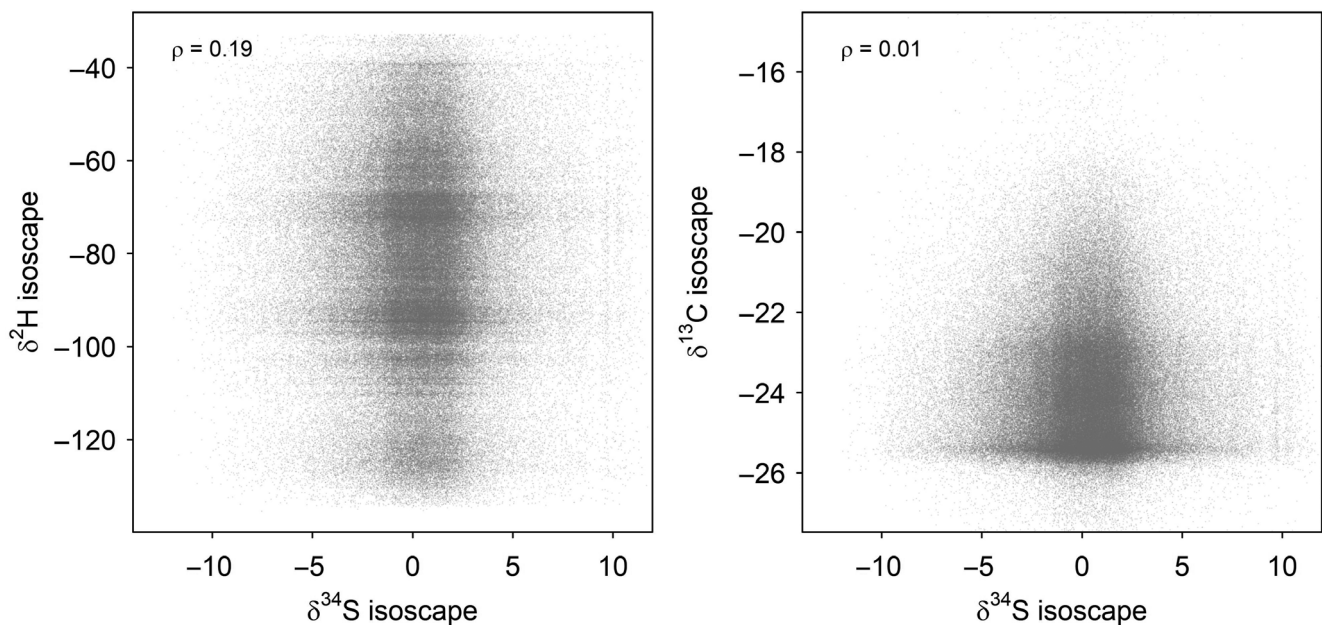


FIGURE 7 Relationships between feather $\delta^{34}\text{S}$ and $\delta^2\text{H}$ isoscapes (left), and feather $\delta^{34}\text{S}$ and $\delta^{13}\text{C}$ isoscapes (right) including Pearson's correlation coefficients.

patches within an individual wetland and regionally among wetlands.

Moreover, our measurements of within-site variability are based on three to four feather samples collected from juvenile Eurasian Reed Warblers during the post-fledgling period at each site. The limited sample sizes could have contributed to large within-site

variation due to stochasticity. Potential post-fledgling dispersals of juvenile Eurasian Reed Warblers between wetlands (Mukhin, 2004) could further increase the variation detected at sampling sites. Similarly, the fledglings or adults feeding them before fledgling could opportunistically use food resources within the wetland as well as in the surrounding terrestrial

habitats with different isotopic signatures adding to the within-site variation in $\delta^{34}\text{S}$ (Catchpole, 1971; Król, 1984).

Complementarity of $\delta^{34}\text{S}$ with other isotopes

Our results showed high complementarity of $\delta^{34}\text{S}$ with other isotopes on both the individual (feather samples) and geographic (isoscape) levels, suggesting different environmental drivers among stable isotopes. However, the high isoscape-level complementarity should be interpreted with caution, primarily because the feather samples used to predict the $\delta^{34}\text{S}$ isoscape in this study were formed in a single habitat type—wetlands, and predictions may not be applicable to different terrestrial habitats. While our results show a high potential of $\delta^{34}\text{S}$ values in Europe, especially in combination with other isotopes, we suggest that a denser sampling of tissues from diverse taxa and across habitats is needed.

CONCLUSIONS

The predicted geographic distribution of $\delta^{34}\text{S}$ values in Europe shows enriched $\delta^{34}\text{S}$ values along the coastline in Europe and slight differences in $\delta^{34}\text{S}$ values between the central and southern parts of Europe. The absence of a systematic spatial pattern, along with observed high within-site variation, limits the sole use of the $\delta^{34}\text{S}$ isoscape. However, the high levels of complementarity on the individual and isoscape levels suggest the potential for combining isoscapes to increase the precision of animal tracing. Therefore, we encourage future studies to focus on the geographic distribution of $\delta^{34}\text{S}$ in homogeneous and large landmasses in Africa, South America, or East Asia. Moreover, we recommend developing a larger database of samples—collected in various environments, habitats, and from different animal species—to support more robust prediction of the geographic distribution of $\delta^{34}\text{S}$. We believe these efforts will significantly advance the knowledge of the $\delta^{34}\text{S}$ geographic distributions and enhance their applications in ecological and forensic studies.

AUTHOR CONTRIBUTIONS

Vojtěch Brlík conceived the idea of the study. Vojtěch Brlík, Frédéric Jiguet, Gergely Osváth, and Petr Procházka collected or provided samples. Luana Bontempo and Federica Camin analyzed stable isotopic composition of samples. Vojtěch Brlík designed the methodology with input from Rebecca L. Powell, Petr Procházka,

Craig A. Stricker, and Michael B. Wunder. Vojtěch Brlík conducted the analyses with input from Michael B. Wunder and Rebecca L. Powell and took the lead in manuscript writing. All authors read, commented, and approved the final version of the manuscript.

ACKNOWLEDGMENTS

We are obliged to the following bird ringers who helped us collect feather samples in Europe: A. Leprêtre, A. Ożarowska, A. Trnka, A. Sponga, A. Pranaitis, B. Vollot, B. Fontaine, B. Bargain, C. Coleiro, R. Galea, C. Z. Martínez, C. Heroguel, C. Ion, D. Vigour, D. Dimitrov, M. Ilieva, D. Ragyov, D. Zhuravlev, D. Leoke, E. Baltag, F. G. Lopez, G. Goujon, J. R. Álvarez, J. Hlaváček, J. J. Baptiste, J. Kralj, J. Reif, J. Beier, J. M. Neto, K. and F. Breek, K. Bedev, K. Bairaktaridau, L. F. P. da Silva, M. Haluzík, M. Šćiban, M. Leconte, M. Olekšák, O. Zakala, P. S. Ranke, P. Matyjasiak, R. Thomas, R. Patapavičius, R. Slobodník, S. Gautier, S. Scebba, S. Capasso, S. Bräger, V. Cohez, V. Fedorov, V. Jusys, W. Fiedler, X. Commecy, Y. Beauvallet, and Z. Karcza. We thank Gabriel Bowen and the Isotopes in Spatial Ecology and Biogeochemistry short course held at the University of Utah for providing the stimulating environment that led to this project. We are also thankful to Carol Kendall for initial advice and reviewers for their comments as well as Andrea Contina for critical comments on this study. Any use of trade, product, or firm names is for descriptive purposes only and does not imply endorsement by the U.S. Government.

FUNDING INFORMATION

This work was supported by the Grant Agency of Charles University (grant no. 254119), Charles University (UNCE 204069), the National Science Foundation (grant no. DBI-1565128), and the Czech Science Foundation (grant no. 20-00648S).

CONFLICT OF INTEREST STATEMENT

The authors declare no conflicts of interest.

DATA AVAILABILITY STATEMENT

Sample metadata are stored and available for reuse in the AviSample Network database (<https://avisample.net/>: AS00001–AS00117; Brlík, Pipek, Brandis, et al., 2022). The information on the isotopic composition and geographic origin of feather samples used to produce the $\delta^{34}\text{S}$ isoscape, predicted feather $\delta^2\text{H}$ (including the geospatial model parameters), $\delta^{13}\text{C}$ and $\delta^{34}\text{S}$ isoscapes (including $\delta^{34}\text{S}$ uncertainty layer), and an annotated R script are available from Zenodo: <https://doi.org/10.5281/zenodo.7315567> (Brlík, Procházka, Bontempo, et al., 2022).

ORCID

Vojtěch Brlík  <https://orcid.org/0000-0002-7902-8123>

Petr Procházka  <https://orcid.org/0000-0001-9385-4547>

Luana Bontempo  <https://orcid.org/0000-0001-7583-1501>

Frédéric Jiguet  <https://orcid.org/0000-0002-0606-7332>

Gergely Osváth  <https://orcid.org/0000-0003-1542-9128>

Craig A. Stricker  <https://orcid.org/0000-0002-5031-9437>

Michael B. Wunder  <https://orcid.org/0000-0002-8063-2408>

Rebecca L. Powell  <https://orcid.org/0000-0002-1978-0153>

REFERENCES

- Abatzoglou, J. T., S. Z. Dobrowski, S. A. Parks, and K. C. Hegewisch. 2018. "TerraClimate, a High-Resolution Global Dataset of Monthly Climate and Climatic Water Balance from 1958–2015." *Scientific Data* 5: 170191.
- Amrani, A., W. Said-Ahmad, Y. Shaked, and R. Kiene. 2013. "Sulfur Isotope Homogeneity of Oceanic DMSP and DMS." *Proceedings of the National Academy of Sciences of the United States of America* 110: 18413–18.
- Amundson, R., A. T. Austin, E. A. G. Schuur, K. Yoo, V. Matzek, C. Kendall, A. Uebersax, D. Brenner, and W. T. Baisden. 2003. "Global Patterns of the Isotopic Composition of Soil and Plant Nitrogen." *Global Biogeochem Cycles* 17: 1031.
- Bataille, C. P., B. E. Crowley, M. J. Wooller, and G. J. Bowen. 2020. "Advances in Global Bioavailable Strontium Isoscapes." *Palaeogeography, Palaeoclimatology, Palaeoecology* 555: 109849.
- Bataille, C. P., K. Jaouen, S. Milano, M. Trost, S. Steinbrenner, É. Crubézy, and R. Colleter. 2021. "Triple Sulfur-Oxygen-Strontium Isotopes Probabilistic Geographic Assignment of Archaeological Remains Using a Novel Sulfur Isoscape of Western Europe." *PLoS One* 16: e0250383.
- Bataille, C. P., I. C. C. von Holstein, J. E. Laffoon, M. Willmes, X.-M. Liu, and G. R. Davies. 2018. "A Bioavailable Strontium Isoscape for Western Europe: A Machine Learning Approach." *PLoS One* 13: e0197386.
- Beck, H. E., N. E. Zimmermann, T. R. McVicar, N. Vergopolan, A. Berg, and E. F. Wood. 2018. "Data Descriptor: Present and Future Köppen-Geiger Climate Classification Maps at 1-km Resolution." *Scientific Data* 5: 180214.
- Belgiu, M., and L. Dragut. 2016. "Random Forest in Remote Sensing: A Review of Applications and Future Directions." *ISPRS Journal Photogrammetry and Remote Sensing* 114: 24–31.
- Bowen, G. J., Z. Liu, H. B. Vander Zanden, L. Zhao, and G. Takahashi. 2014. "Geographic Assignment with Stable Isotopes in IsoMAP." *Methods Ecology Evolution* 5: 201–6.
- Bowen, G. J., and J. Revenaugh. 2003. "Interpolating the Isotopic Composition of Modern Meteoric Precipitation." *Water Resources Research* 39: 1–13.
- Breiman, L. 2001. "Random Forests." *Machine Learning* 45: 5–32.
- Brlík, V., P. Pipek, K. Brandis, N. Chernetsov, M. Herrera, F. J. Costa, L. G. Herrera M, et al. 2022. "The Reuse of Avian Samples: Opportunities, Pitfalls, and a Solution." *Ibis* 164: 343–49.
- Brlík, V., P. Procházka, L. Bontempo, F. Camin, F. Jiguet, G. Osváth, C. Stricker, M. Wunder, and R. Powell. 2022. "Spatial Distribution of Feather Sulfur Isotopes in Europe." Zenodo. <https://doi.org/10.5281/zenodo.7315567>.
- Brlík, V., P. Procházka, B. Hansson, C. A. Stricker, E. Yohannes, R. L. Powell, and M. B. Wunder. 2022. "Animal Tracing with Sulfur Isotopes: Spatial Segregation and Climate Variability in Africa Likely Contribute to Population Trends of a Migratory Songbird." *Journal of Animal Ecology* 92: 1320–31.
- Buchhorn, M., M. Lesiv, N.-E. Tsendbazar, M. Herold, L. Bertels, and B. Smets. 2020. "Copernicus Global Land Cover Layers—Collection 2." *Remote Sensing* 12: 1044.
- Case, J. W., and H. R. Krouse. 1980. "Variations in Sulphur Content and Stable Sulphur Isotope Composition of Vegetation near a SO₂ Source at Fox Creek, Alberta, Canada." *Oecologia* 257: 248–257.
- Catchpole, C. K. 1971. "A Comparative Study of Territory in the Reed Warbler (*Acrocephalus scirpaceus*) and Sedge Warbler (*A. schoenobaenus*)." *Journal of Zoology* 166: 213–231.
- Chambers, L., and P. Trudinger. 1979. "Microbiological Fractionation of Stable Sulfur Isotopes: A Review and Critique." *Geomicrobiology Journal* 1: 249–293.
- Cherry, J. 2011. "Ecology of Wetland Ecosystems: Water, Substrate, and Life." *Nature Education Knowledge* 3: 16.
- CIESIN. 2018. *Gridded Population of the World, Version 4 (GPWv4): Population Density, Revision 11*. Palisades, NY: NASA Socioeconomic Data and Applications Center (SEDAC). <https://doi.org/10.7927/H49C6VHW>.
- Contina, A., S. Magozzi, H. B. Vander Zanden, G. J. Bowen, and M. B. Wunder. 2022. "Optimizing Stable Isotope Sampling Design in Terrestrial Movement Ecology Research." *Methods in Ecology and Evolution* 13: 1237–49.
- Copernicus Sentinel. 2015a. "Sentinel-5P NRTI SO₂: Near Real-Time Sulphur Dioxide." https://developers.google.com/earth-engine/datasets/catalog/COPERNICUS_S5P_NRTI_L3_SO2.
- Copernicus Sentinel. 2015b. "Sentinel-5P NRTI NO₂: Near Real-Time Nitrogen Dioxide." https://developers.google.com/earth-engine/datasets/catalog/COPERNICUS_S5P_NRTI_L3_NO2.
- Danielson, J., and D. Gesch. 2011. "Global Multi-Resolution Terrain Elevation Data." USGS Report: 1073.
- Dansgaard, W. 1954. "The O18-Abundance in Fresh Water." *Geochimica et Cosmochimica Acta* 6: 241–260.
- Dansgaard, W. 1964. "Stable Isotopes in Precipitation." *Tellus* 16: 436–468.
- Felicetti, L. A., C. C. Schwartz, R. O. Rye, M. A. Haroldson, K. A. Gunther, D. L. Phillips, and C. T. Robbins. 2003. "Use of Sulfur and Nitrogen Stable Isotopes to Determine the Importance of Whitebark Pine Nuts to Yellowstone Grizzly Bears." *Canadian Journal of Zoology* 81: 763–770.
- Florin, S. T., L. A. Felicetti, and C. T. Robbins. 2011. "The Biological Basis for Understanding and Predicting Dietary-Induced Variation in Nitrogen and Sulphur Isotope Ratio Discrimination." *Functional Ecology* 25: 519–526.
- Fry, B. 2006. *Stable Isotopes Ecology*. New York: Springer.
- Garg, A., P. R. Shukla, S. Bhattacharya, and V. K. Dadhwal. 2001. "Sub-Region (District) and Sector Level SO₂ and NO_x Emissions for India: Assessment of Inventories and Mitigation Flexibility." *Atmospheric Environment* 35: 703–713.
- Gorelick, N., M. Hancher, M. Dixon, S. Ilyushchenko, D. Thau, and R. Moore. 2017. "Google Earth Engine: Planetary-Scale

- Geospatial Analysis for Everyone.” *Remote Sensing of the Environment* 202: 18–27.
- Grinkevich, V., N. Chernetsov, and A. Mukhin. 2009. “Juvenile Reed Warblers *Acrocephalus scirpaceus* See the World but Settle Close to Home.” *Avian Ecology Behaviour* 16: 3–10.
- Hobson, K. A., S. L. Van Wilgenburg, L. I. Wassenaar, R. L. Powell, C. J. Still, and J. M. Craine. 2012. “A Multi-Isotope ($\delta^{13}\text{C}$, $\delta^{15}\text{N}$, $\delta^2\text{H}$) Feather Isoscape to Assign Afrotropical Migrant Birds to Origins.” *Ecosphere* 3: 44.
- Hobson, K. A., and L. I. Wassenaar. 2018. *Tracking Animal Migration with Stable Isotopes*. London: Academic Press.
- Jiguet, F., A. Robert, R. Lorrillière, K. A. Hobson, K. J. Kardynal, R. Arlettaz, F. Bairlein, et al. 2019. “Unravelling Migration Connectivity Reveals Unsustainable Hunting of the Declining Oortolan Bunting.” *Science Advances* 5: eaau2642.
- Kabalika, Z., T. A. Morrison, R. A. R. McGill, L. K. Munishi, D. Ekwem, W. L. Mahene, A. L. Lobora, et al. 2020. “Tracking Animal Movements Using Biomarkers in Tail Hairs: A Novel Approach for Animal Geolocating from Sulfur Isoscapes.” *Movement Ecology* 8: 37.
- Król, A. 1984. “Wykluczanie się żerowisk samca i samicy trzcinniczka (*Acrocephalus scirpaceus*) w okresie karmienia piskląt.” *Dolina Baryczy* 3: 48–53.
- Kuhn, M. 2008. “Building Predictive Models in R Using the Caret Package.” *Journal Statistical Software* 28: 1–26.
- Lott, C. A., T. D. Meehan, and J. A. Heath. 2003. “Estimating the Latitudinal Origins of Migratory Birds Using Hydrogen and Sulfur Stable Isotopes in Feathers: Influence of Marine Prey Base.” *Oecologia* 134: 505–510.
- Martin, R. V., D. J. Jacob, K. Chance, T. P. Kurosu, P. I. Palmer, and M. J. Evans. 2003. “Global Inventory of Nitrogen Oxide Emissions Constrained by Space-Based Observations of NO_2 Columns.” *Journal of Geophysical Research* 108: 4537.
- McCutchan, J. H., W. M. Lewis, C. Kendall, and C. C. Mcgrath. 2003. “Variation in Trophic Shift for Stable Isotope Ratios of Carbon, Nitrogen, and Sulfur.” *Oikos* 2: 378–390.
- Mukhin, A. 2004. “Night Movements of Young Reed Warblers (*Acrocephalus scirpaceus*) in Summer: Is It Postfledging Dispersal?” *Auk* 121: 203–9.
- NASA Ocean Biology Processing Group. 2012. “Distance to Nearest Coastline: 0.01-Degree Grid.” <https://catalog.data.gov/dataset/distance-to-nearest-coastline-0-01-degree-grid-ocean>.
- Newton, J. 2021. “An Insect Isoscape of UK and Ireland.” *Rapid Communications in Mass Spectrometry* 35: e9126.
- Norris, D. R., P. P. Marra, G. J. Bowen, L. M. Ratcliffe, J. A. Royle, and T. K. Kyser. 2006. “Migratory Connectivity of a Widely Distributed Songbird, the American Redstart (*Setophaga ruticilla*).” *Ornithological Monographs* 61: 14–28.
- Ohizumi, T., and N. Fukuzaki. 1997. “Sulphur Isotopic View on the Sources of Sulphur in Atmospheric Fallout along the Coast of the Sea of Japan.” *Atmospheric Environment* 31: 1339–48.
- Pawlewicz, M. J., A. J. Williams, S. M. Walden, and D. W. Steinshouer. 2003. “Generalized Geology of Europe Including Turkey.” USGS.
- Popa-Lisseanu, A. G., K. Sörgel, A. Luckner, L. I. Wassenaar, C. Ibáñez, S. Kramer-Schadt, M. Ciechanowski, et al. 2012. “A Triple-Isotope Approach to Predict the Breeding Origins of European Bats.” *PLoS One* 7: e30388.
- Powell, R., S. Firmin, and D. Griffith. 2019. “grassmapr, an R Package to Predict C3/C4 Grass Distributions and Model Terrestrial $\delta^{13}\text{C}$ Isoscapes.” <https://github.com/rebeccapowell/grassmapr>.
- Powell, R. L., and C. J. Still. 2010. “Continental-Scale Distributions of Vegetation Stable Carbon Isotope Ratios.” In *Isoscapes*, edited by J. B. West, G. J. Bowen, T. E. Dawson, and K. P. Tu, 495. Dordrecht: Springer.
- Powell, R. L., E.-H. Yoo, and C. J. Still. 2012. “Vegetation and Soil Carbon-13 Isoscapes for South America: Integrating Remote Sensing and Ecosystem Isotope Measurements.” *Ecosphere* 3: 109.
- Procházka, P., V. Brlik, E. Yohannes, B. Meister, M. Ilieva, and S. Hahn. 2018. “Across a Migratory Divide: Divergent Migration Directions and Non-Breeding Grounds of Eurasian Reed Warblers Revealed by Geolocators and Stable Isotopes.” *Journal of Avian Biology* 49: e01769.
- Procházka, P., S. L. Van Wilgenburg, J. M. Neto, R. Yosef, and K. A. Hobson. 2013. “Using Stable Hydrogen Isotopes ($\delta^2\text{H}$) and Ring Recoveries to Trace Natal Origins in a Eurasian Passerine with a Migratory Divide.” *Journal of Avian Biology* 44: 541–550.
- R Core Team. 2021. *A Language and Environment for Statistical Computing*. Vienna: R Foundation for Statistical Computing.
- Rees, C., W. Jenkins, and J. Monster. 1978. “The Sulphur Isotopic Composition of Ocean Water Sulphate.” *Geochimica et Cosmochimica Acta* 42: 377–381.
- Tcherkez, G., and I. Tea. 2013. “ $^{32}\text{S}/^{34}\text{S}$ Isotope Fractionation in Plant Sulphur Metabolism.” *New Phytologist* 200: 44–53.
- Thode, H. G. 1991. “Sulphur Isotopes in Nature and the Environment: An Overview.” In *Stable Isotopes in the Assessment of Natural and Anthropogenic Sulphur in the Environment*, edited by H. R. Krouse and V. A. Grinenko, 1–26. Chichester: Wiley.
- Thode, H. G., J. Macnamar, and W. Fleming. 1953. “Sulphur Isotope Fractionation in Nature and Geological and Biological Time Scales.” *Geochimica et Cosmochimica Acta* 3: 235–243.
- Troen, I., and E. Petersen. 1989. *European Wind Atlas*. Roskilde: Riso National Laboratory.
- Valenzuela, L. O., L. A. Chesson, S. P. O’Grady, T. E. Cerling, and J. R. Ehleringer. 2011. “Spatial Distributions of Carbon, Nitrogen and Sulfur Isotope Ratios in Human Hair across the Central United States.” *Rapid Communications in Mass Spectrometry* 25: 861–68.
- Vapnik, V. N. 1998. *Statistical Learning Theory*. New York: Wiley.
- Veen, T., B. Hjærnquist, S. L. Van Wilgenburg, K. A. Hobson, E. Folmer, L. Font, and M. Klaassen. 2014. “Identifying the African Wintering Grounds of Hybrid Flycatchers Using a Multi-Isotope ($\delta^2\text{H}$, $\delta^{13}\text{C}$, $\delta^{15}\text{N}$) Assignment Approach.” *PLoS One* 9: e98075.
- Villegas, M., S. D. Newsome, and J. G. Blake. 2016. “Seasonal Patterns in $\delta^2\text{H}$ Values of Multiple Tissues from Andean Birds Provide Insights into Elevational Migration.” *Ecological Applications* 26: 2383–89.
- Wadleigh, M. A., and D. M. Blake. 1999. “Tracing Sources of Atmospheric Sulphur Using Epiphytic Lichens.” *Environmental Pollution* 106: 265–271.
- West, J. B., G. J. Bowen, T. E. Dawson, and K. P. Tu. 2010. *Isoscapes*. New York: Springer.
- Yu, Q., L. You, U. Wood-Sichra, Y. Ru, A. K. B. Joglekar, S. Fritz, W. Xiong, M. Lu, W. Wu, and P. Yang. 2020. “A Cultivated

Planet in 2010: 2. The Global Gridded Agricultural Production Maps." *Earth System Science Data* 12: 1–40.

Zazzo, A., F. J. Monahan, A. P. Moloney, S. Green, and O. Schmidt. 2011. "Sulphur Isotopes in Animal Hair Track Distance to Sea." *Rapid Communications in Mass Spectrometry* 25: 2371–78.

SUPPORTING INFORMATION

Additional supporting information can be found online in the Supporting Information section at the end of this article.

How to cite this article: Brlík, Vojtěch, Petr Procházka, Luana Bontempo, Federica Camin, Frédéric Jiguet, Gergely Osváth, Craig A. Stricker, Michael B. Wunder, and Rebecca L. Powell. 2024. "Geographic Distribution of Feather $\delta^{34}\text{S}$ in Europe." *Ecosphere* 15(2): e4690. <https://doi.org/10.1002/ecs2.4690>